The Astronomical Journal, 143:5 (8pp), 2012 January doi:10.1088/0004-6256/143/1/5

ABSOLUTE PROPERTIES OF THE HIGHLY ECCENTRIC, SOLAR-TYPE ECLIPSING BINARY HD 74057

James R. Sowell[1], Gregory W. Henry[2], and Francis C. Fekel[2,3]
[1] School of Physics, Georgia Institute of Technology, Atlanta, GA 30332, USA; jim.sowell@physics.gatech.edu
[2] Center of Excellence in Information Systems, Tennessee State University, 3500 John A. Merritt Boulevard, Box 9501, Nashville, TN 37209, USA; gregory.w.henry@gmail.com, fekel@evans.tsuniv.edu
Received 2011 August 25; accepted 2011 October 31; published 2011 November 29

ABSTRACT

We have obtained Strömgren *b* and *y* differential photometric observations of the solar-type eclipsing binary HD 74057 plus follow-up high-resolution, red wavelength spectroscopic observations. The system has an orbital period of 31.2198 days, a high eccentricity of 0.47, and is seen almost exactly edge on with an inclination of 89.°8. The two main-sequence G0 stars are nearly identical in all physical characteristics. We used the Wilson–Devinney program to obtain a simultaneous solution of our photometric and spectroscopic observations. The resulting masses of the components are $M_1 = 1.138 \pm 0.003\,M_\odot$ and $M_2 = 1.131 \pm 0.003\,M_\odot$, and the radii are $R_1 = 1.064 \pm 0.002\,R_\odot$ and $R_2 = 1.049 \pm 0.002\,R_\odot$. The effective temperatures are 5900 K (fixed) and 5843 K, and the iron abundance, [Fe/H], is estimated to be +0.07. A comparison with evolutionary tracks suggests that the system may be even more metal rich. The components rotate with periods of 8.4 days, significantly faster than the predicted pseudosynchronous period of 12.7 days. We see evidence that one or both components have cool spots. Both stars are close to the zero-age main sequence and are about 1.0 Gyr old.

Key words: binaries: close – binaries: eclipsing – binaries: spectroscopic

Online-only material: color figures, machine-readable and VO tables

1. INTRODUCTION

HD 74057 = HIP 42753 ($\alpha = 08^h42^m45^s.90$, $\delta = 31°51'41''.0$ (2000)) was an undistinguished seventh magnitude late-F star in northern Cancer until Davies (2006) examined the data from an automated survey for variable stars and discovered it to be an eclipsing binary. He collected additional eclipse observations (Davies 2007) and found the primary and secondary eclipses to have similar depths (∼50%) but very different durations (5.45 and 13.53 hr, respectively). He determined an orbital period of 31.2198 days and concluded that the two components have similar mass, size, and brightness and, furthermore, that the orbit has a large eccentricity of 0.6 and an inclination very close to 90°.

We began observing HD 74057 in 2001 when we added it to our photometric program designed to detect long-term spot cycles in solar-type stars (Henry 1999). It was selected as a mildly active star, based on its log R'_{HK} value of −4.5, provided to us by D. Soderblom (2001, private communication). We independently discovered its eclipses and began spectroscopic observations in 2002. In this paper, we present our photometric and spectroscopic observations of HD 74057 as well as a detailed analysis of the light and radial velocity curves, which enable us to determine fundamental properties of this double-lined binary. We then compare the properties of the components with Yonsei-Yale evolutionary tracks.

2. PHOTOMETRIC OBSERVATIONS AND REDUCTIONS

Our photometric observations of HD 74057 were acquired during its 2001–2002 and 2004–2005 observing seasons with the T10 0.80 m automatic photometric telescope (APT) located at Fairborn Observatory in the Patagonia Mountains of southern Arizona. The T10 APT is nearly identical to the T8 0.80 m APT described in Henry (1999). Like the T8 APT, T10 has a two-channel precision photometer that uses a dichroic beam splitter to enable the simultaneous measurement of the Strömgren *b* and *y* passbands with separate EMI 9124QB bi-alkali photomultiplier tubes (PMTs). The APT measures the difference in brightness between a program star and a nearby constant comparison star or stars with a typical precision of ∼0.0015 mag for single measurements of bright stars ($V \lesssim 8.5$).

We used the T10 APT to make single, night-to-night observations of HD 74057 throughout both the 2001–2002 and 2004–2005 observing seasons to establish the out-of-eclipse light level of the system. We also used T10 to make higher-cadence monitoring observations of the primary and secondary eclipses during six nights of the 2004–2005 observing season. The resulting data are described in the following two subsections.

2.1. Out-of-eclipse Photometry

We acquired 99 and 68 nightly brightness measurements of HD 74057 during the 2001–2002 and 2004–2005 observing seasons, respectively. The telescope was programmed to measure the brightness of HD 74057 with respect to three nearby comparison stars in the following sequence: DARK, A, B, C, D, A, SKY_A, B, SKY_B, C, SKY_C, D, SKY_D, A, B, C, D. The comparison stars A, B, and C are HD 73596 ($V = 6.21$, $B - V = 0.40$, F5 III), HD 72114 ($V = 7.79$, $B-V = 0.41$, F2), and HD 71277 ($V = 8.18$, $B - V = 0.41$, F2), respectively, while star D is HD 74057 ($V = 7.18$, $B - V = 0.60$, F8).

Each complete sequence, referred to as a group observation, was reduced to form three independent measures of each of the six differential magnitudes D−A, D−B, D−C, C−A, C−B, and B−A. The differential magnitudes were corrected for differential extinction with nightly extinction coefficients and transformed to the standard Strömgren system with yearly mean transformation coefficients. The three independent measures of each differential magnitude within each group observation

[3] Visiting Astronomer, Kitt Peak National Observatory, National Optical Astronomy Observatory, operated by the Associated Universities for Research in Astronomy, Inc., under cooperative agreement with the National Science Foundation.

Table 1
Photometric Observations[a]

Heliocentric Julian Date (HJD − 2,400,000)	Phase	Δy	Δb
52,196.9886	0.0353	+0.983	+1.093
52,197.9775	0.0669	+0.983	+1.094
52,198.9815	0.0991	+0.984	+1.093
52,200.9715	0.1628	+0.976	+1.084
52,203.9680	0.2588	+0.981	+1.089

Note. [a] The phases are based on parameter values listed in Table 6.

(This table is available in its entirety in machine-readable and Virtual Observatory (VO) forms in the online journal. A portion is shown here for guidance regarding its form and content.)

were combined, giving one mean data point per complete sequence for each of the six differential magnitudes. If the standard deviation of any of the six mean differential magnitudes exceeded 0.01 mag, the entire group observation was discarded to filter observations taken under non-photometric conditions.

The scatter of all 167 out-of-eclipse C−A, C−B, and B−A differential magnitudes of the three comparison stars, as measured by the standard deviation of a single observation from the mean, was within the range 0.0014–0.0018 mag for both the Strömgren b and y observations. Periodogram analyses of these comparison star differential magnitudes failed to reveal any significant periodicity between 1 and 100 days. Thus, all three of our comparison stars are constant to the limit of precision for a single observation. We chose to use the D−A differential magnitudes in b and y for our light curve analyses.

The 2001–2002 and 2004–2005 nightly (D−A) out-of-eclipse observations are presented as the first 167 rows of Table 1. The times in Table 1 are heliocentric Julian dates (HJD); the HJDs for each nightly Δb and Δy observation are identical since the two bands were measured simultaneously. The Δy measurements from the two observing seasons are plotted separately in the top panels of Figures 1 and 2. The mean Δy light levels of each season are shown in the top panels by the horizontal dashed lines; the two means are identical within their uncertainties. The scatter (standard deviation) of the observations in the first and second observing seasons is 0.0043 and 0.0032 mag, respectively. These values are significantly greater than the ∼0.0015 mag measurement precision, suggesting that star D (HD 74057) exhibits low-amplitude, out-of-eclipse brightness variability.

Periodogram analyses of the two seasons (based on least-squares fitting of sine curves) are shown in the middle panels of Figures 1 and 2, where we plot the fractional reduction of the total variance (reduction factor) of the data versus trial frequency.

The corresponding best-fit periods are 8.49 and 4.26 days for 2001–2002 and 2004–2005, respectively. We interpret the 8.49 day period as the stellar rotation period, made apparent by rotational modulation of starspots on the stellar photosphere. The photometric period in the second season is 4.26 days, exactly half (within the uncertainties) of the rotation period found in the first season. A continually increasing amplitude and a brightness trend are also seen in the second season. We interpret these changes as a result of ongoing redistribution of the spot activity on the stellar surface, either through differential rotation and/or the growth and decay of individual spot regions. The halving of the photometric period between the two observing seasons is a consequence of the redistribution of spots to opposite hemispheres of the stellar surface, which

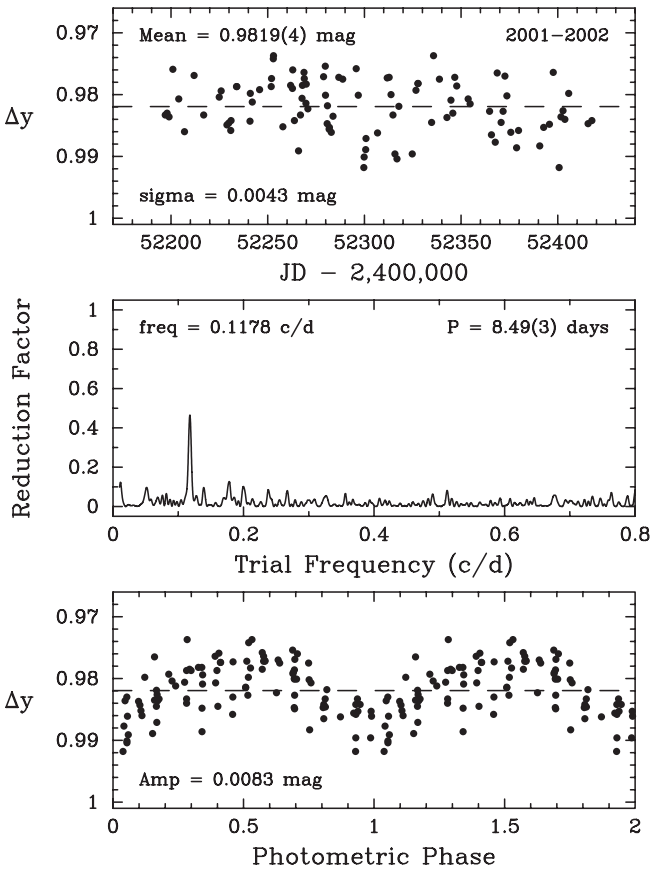

Figure 1. Top: nightly Strömgren Δy magnitudes from the T10 APT for the 2001–2002 observing season. Middle: frequency spectrum of the Δy observations showing the best-fit period of 8.49 days, which we take to be the rotation period of the active component(s). Bottom: Δy observations phased with the 8.49 day rotation period have an amplitude of 0.008 mag. The horizontal dashed lines in the top and bottom panels represent the mean brightness of the Δy data set.

results in two brightness maxima and two minima per stellar rotation. Phase curves of the two observing seasons computed with the 8.49 and 4.26 day periods are plotted in the bottom panels of Figures 1 and 2, respectively. Least-squares sine fits of the two phase curves give peak-to-peak amplitudes of 0.0083 and 0.0049 mag, respectively. The changing spot amplitude in the second season is another effect of spot redistribution. The photometric variability in HD 74057 is typical of that seen in other low-amplitude, starspot variables (e.g., Henry et al. 1995).

This simple depiction of starspot activity is complicated by the fact that HD 74057 is an eccentric double-lined binary with very similar components, as we show below by modeling the light and velocity curves. Therefore, because we cannot identify whether the primary or the secondary component of the binary (or both) is the active component, we cannot rectify the light curve to remove the effects of the spots. However, since the eclipse amplitudes are *several hundred times* larger than the spot variations, we can safely ignore the spot variability in our light curve solutions below.

2.2. Eclipse Photometry

On six nights during the 2004–2005 observing season, we used the T10 APT to acquire higher-cadence observations for several hours each night during primary and secondary eclipse. The APT was programmed to observe HD 74057 differentially with respect to the single comparison star A (HD 73596). Each

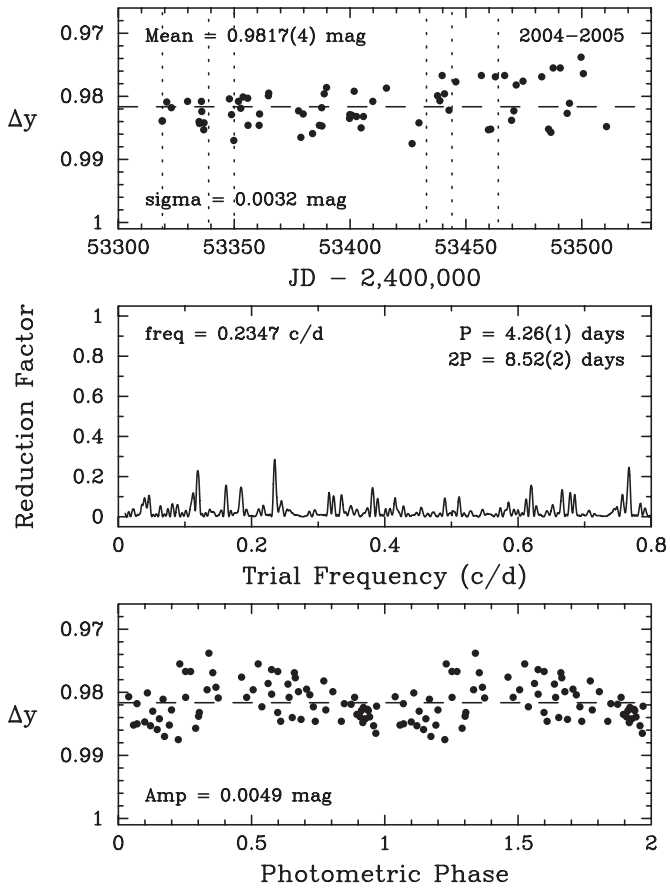

Figure 2. Top: nightly Strömgren Δy magnitudes from the T10 APT for the 2004–2005 observing season. The vertical dotted lines mark the JDs of the eclipse monitoring nights. Middle: frequency spectrum of the Δy observations showing the best-fit period of 4.26 days, which we take to be half the stellar rotation period. Bottom: Δy observations phased with the 4.26 day period have an amplitude of only 0.005 mag. The horizontal dashed lines in the top and bottom panels represent the mean brightness of the Δy data set.

individual differential magnitude (D−A) is treated as a single observation. Measurements on three of the six monitoring nights covered the primary eclipse; the other three nights covered most of the secondary eclipse. A total of 1067 differential magnitudes was acquired on these six nights. They are listed in Table 1, immediately after the out-of-eclipse observations and are used in our light curve solutions below. The six monitoring nights are indicated by the vertical dotted lines in the top panel of Figure 2.

3. SPECTROSCOPIC OBSERVATIONS AND REDUCTIONS

From 2002 February to 2007 June, 27 observations, obtained at double-lined phases, were acquired with the Coudé feed telescope, Coudé spectrograph, and a TI CCD detector at the Kitt Peak National Observatory (KPNO). The spectrograms are centered at 6430 Å, cover a wavelength range of 84 Å, and have a resolution of 0.21 Å. The signal-to-noise ratio is typically about 150.

Radial velocities were determined with the IRAF cross-correlation program FXCOR (Fitzpatrick 1993). Two International Astronomical Union radial-velocity standard stars, β Vir and 10 Tau, having adopted velocities of 4.4 and 27.9 km s^{-1} (Scarfe et al. 1990), respectively, were used as cross-correlation reference stars. Table 2 gives the HJDs of mid-observation and the corresponding radial velocities of the primary and secondary components. Additionally, that table lists the fractional phases of the observations, computed from a time of periastron, and the residuals to the orbit, both from the spectroscopic solution discussed below.

4. SPECTROSCOPIC ORBIT

We adopted a preliminary eclipse period of 31.22 days and computed an orbital solution of the primary, component 1, with BISP (Wolfe et al. 1967), a computer program that implements a slightly modified version of the Wilsing–Russell method. That orbital solution was then refined with SB1 (Barker et al. 1967), a program that uses differential corrections. We determined an orbit for the secondary, component 2, in the same manner. Because the variances of the solutions for the primary and secondary were similar, we assigned unit weights to all velocities of both components. Finally, the spectroscopic orbits of the primary and secondary were recomputed with a version of SB1 that was modified to simultaneously analyze both components. The orbital elements and derived quantities from that spectroscopic solution are presented in Table 3.

5. COMBINED LIGHT AND VELOCITY SOLUTION

Light and velocity solutions were computed with the 2003 version of the Wilson–Devinney (WD) program. The program's physical model is described in detail in Wilson & Devinney (1971) and Wilson (1979, 1990). It now includes an improved stellar atmosphere treatment (Van Hamme & Wilson 2003), which is based on pre-fitted Legendre functions to Kurucz (1993) atmosphere models.

Simultaneous photometric and double-lined radial velocity solutions were obtained to improve parameter consistency (Wilson 1979; Van Hamme & Wilson 1984, 1985). Curve-dependent weights were based on the standard deviations that are listed in Table 4. Light-level-dependent weights were applied inversely proportional to the square root of the light level. A square-root limb-darkening law was adopted with coefficients x, y from Van Hamme (1993) and, due to the large separation of the stars, the treatment of reflection from Wilson (1990) was used with only one reflection. Gravity darkening (g) and bolometric albedo (A) coefficients were fixed at convective-envelope, canonical values of Lucy (1967). We utilized the improved atmosphere model option. Values of these non-varying parameters are listed in Table 5.

The temperatures could not be implied by existing MK spectral classifications for none were found in the literature. Instead, we established an effective temperature for the primary by using the observed $B - V = 0.598$ from the *Hipparcos* catalog and the [Fe/H] value of +0.07 from the stars that best fit our HD 74057 spectra, as determined below. We input those values into the $T_e - (B - V) - [\mathrm{Fe/H}]$ temperature scale (i.e., Equation (1)) of Alonso et al. (1996). The resulting mean temperature for the binary pair is 5874 K. For comparison, Flower (1996), who determined an empirical scale between effective temperature and $B - V$ color, gives $T_e = 5891$ K for $B - V = 0.60$. Thus, we initially adopted $T_e = 5900$ K for the primary, which was held constant. After a solution was obtained, the WD program was re-run with temperatures of 5800 K and 6000 K, but in both cases the sum of the squares of the residuals was higher than in the 5900 K solution. Although the WD program computes a very small, formal error for the secondary's effective temperature, we estimate the error for both temperatures to be ±100 K.

Table 2
Radial Velocities[a]

Heliocentric Julian Date (HJD − 2,400,000)	Phase	V_1 (km s^{-1})	$(O-C)_1$ (km s^{-1})	V_2 (km s^{-1})	$(O-C)_2$ (km s^{-1})
52,327.831	0.251	−30.8	0.4	41.8	0.2
52,330.824	0.347	−23.4	−0.4	33.6	0.3
52,390.662	0.263	−30.0	0.3	40.8	0.1
52,394.632	0.390	−18.9	−0.2	29.3	0.3
52,395.666	0.423	−15.8	−0.5	25.4	−0.1
52,705.782	0.357	−22.3	−0.2	32.1	−0.2
52,755.693	0.955	63.2	0.0	−53.8	0.0
52,756.688	0.987	48.3	0.4	−38.3	0.0
52,757.691	0.019	19.6	−0.1	−9.5	0.3
52,758.651	0.050	−5.7	0.1	15.7	−0.2
52,759.690	0.083	−23.2	−0.3	33.5	0.3
52,760.712	0.116	−31.0	0.1	41.7	0.3
52,942.012	0.923	64.5	−0.4	−55.6	−0.1
53,121.644	0.677	16.7	−0.1	−6.7	0.1
53,123.692	0.743	27.7	−0.2	−18.4	−0.3
53,487.636	0.400	−18.1	−0.4	28.3	0.3
53,635.018	0.121	−32.0	−0.2	42.0	−0.1
53,636.013	0.153	−34.5	−0.2	44.5	−0.2
53,637.018	0.185	−34.4	0.1	44.7	−0.2
53,638.021	0.217	−33.4	−0.1	43.6	−0.1
53,852.664	0.092	−25.8	0.0	36.3	0.1
53,856.686	0.221	−32.9	0.2	43.4	−0.1
54,002.021	0.876	56.6	0.0	−47.0	0.1
54,005.019	0.972	56.9	−0.2	−47.6	0.0
54,221.673	0.912	63.8	0.2	−53.7	0.4
54,223.664	0.976	55.4	0.1	−45.8	0.0

Note. [a] Phases and $(O-C)$ residuals are computed with the spectroscopic values presented in Table 3.

Table 3
Spectroscopic Orbital Elements[a]

Parameter	Value
P (days)	31.21987 ± 0.00015
T (HJD)	2,453,100.5029 ± 0.0081
γ (km s^{-1})	5.012 ± 0.035
K_1 (km s^{-1})	50.039 ± 0.065
K_2 (km s^{-1})	50.522 ± 0.065
e	0.46721 ± 0.00075
ω_1 (deg)	63.59 ± 0.13
$a_1 \sin i$ (10^6 km)	18.993 ± 0.026
$a_2 \sin i$ (10^6 km)	19.177 ± 0.026
$m_1 \sin^3 i$ ($M_\odot$)	1.1423 ± 0.0034
$m_2 \sin^3 i$ ($M_\odot$)	1.1314 ± 0.0034

Note. [a] Solution computed from spectroscopic data alone.

Table 4
Measurement Characteristics

Curve	Data Points	Normal Mag	σ[a]
Strömgren y	1234	7.190	0.003
Strömgren b	1234	7.568	0.003
RV_1	27	...	0.35 km s^{-1}
RV_2	27	...	0.31 km s^{-1}

Note. [a] For the light curves, in units of total light at phase 0.25.

We used Mode 2 of the WD program since this provides more degrees of freedom. The resulting orbital elements are given in Table 6. Figure 3 shows the observed measurements along with the light curves computed in each bandpass from our orbital elements. For clarity, expanded views of the primary and secondary eclipses are shown in Figures 4 and 5, respectively.

Table 5
Non-varying WD Parameters

Parameter	Symbol	Value
Rotation/orbit ratio	F_1, F_2	1.0, 1.0
Albedo (bolo)	A_1, A_2	0.30, 0.30
Gravity darkening	g_1, g_2	0.30, 0.30
Limb darkening (bolo)	x_1, y_1	+0.159, +0.559
Limb darkening (bolo)	x_2, y_2	+0.159, +0.559
Limb darkening (y)	x_1, y_1	+0.187, +0.642
Limb darkening (y)	x_2, y_2	+0.187, +0.642
Limb darkening (b)	x_1, y_1	+0.342, +0.546
Limb darkening (b)	x_2, y_2	+0.342, +0.546

The individual radial velocities are compared with the computed curve in Figure 6. The observations were obtained at orbital phases well outside of the eclipses, so the Rossiter effect (Rossiter 1924) was not observed.

The two components have expected absolute dimensions for the parameter values and constraints used. The masses are $M_1 = 1.138 \pm 0.003\ M_\odot$ and $M_2 = 1.131 \pm 0.003\ M_\odot$, and the radii are $R_1 = 1.064 \pm 0.002\ R_\odot$ and $R_2 = 1.049 \pm 0.002\ R_\odot$. The absolute dimensions are provided in Table 7. The surface temperatures, masses, and radii of the components are similar to those of G0 V stars (Allen 2000).

6. ECLIPSE EPHEMERIDES

For the light and velocity curve solutions described in Section 5, we used time (HJD) instead of phase as the independent variable. This allowed us to determine ephemeris parameters, reference epoch T_0 (i.e., the time of primary eclipse minimum) and period P, as part of the solution. These

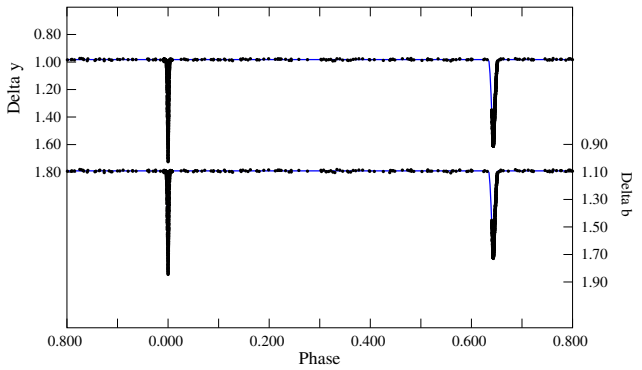

Figure 3. Differential Strömgren *b* and *y* magnitudes of HD 74057 plotted with the Wilson–Devinney solution curves.

(A color version of this figure is available in the online journal.)

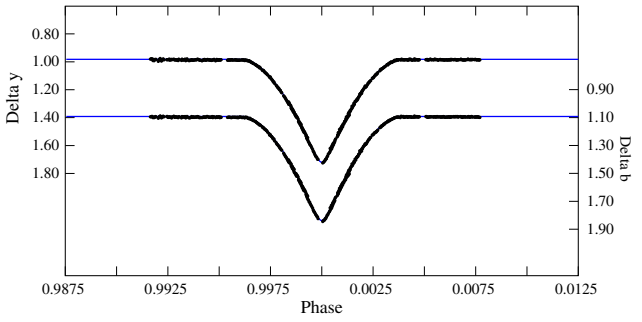

Figure 4. Expanded view of the differential Strömgren *b* and *y* magnitudes of HD 74057 during primary eclipse plotted with the Wilson–Devinney solution curves.

(A color version of this figure is available in the online journal.)

parameters are now based on whole curves, not just on times of minimum.

For our new eclipse ephemerides, we define the time of mid-primary eclipse as phase 0.0:

$$\text{Minimum Light (HJD)} = 2{,}454{,}162.73553 \pm 0.00002 + 31.2197874 \pm 0.0000014\, E \text{ days}.$$

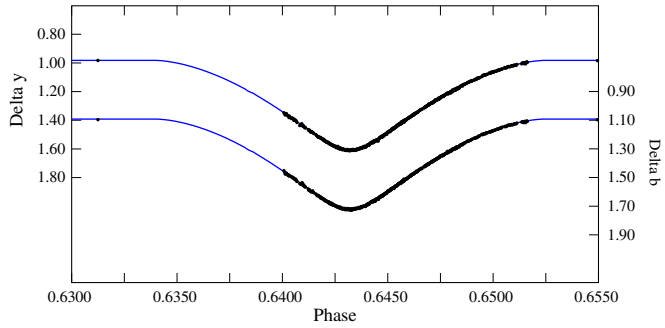

Figure 5. Expanded view of the differential Strömgren *b* and *y* magnitudes of HD 74057 during secondary eclipse plotted with the Wilson–Devinney solution curves.

(A color version of this figure is available in the online journal.)

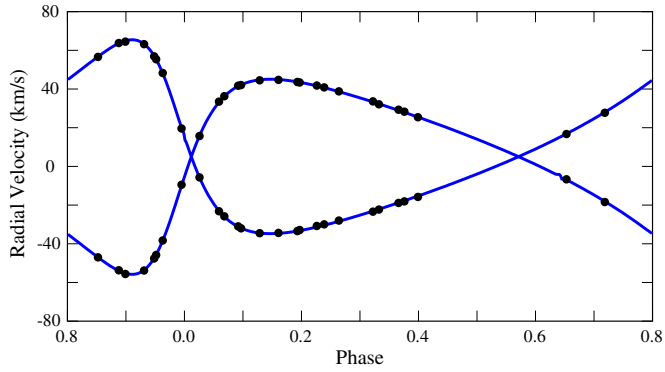

Figure 6. Radial velocities of HD 74057 plotted with the Wilson–Devinney solution curves.

(A color version of this figure is available in the online journal.)

The time of secondary minimum then occurs at phase of 0.64325.

$$\text{Minimum Light (HJD)} = 2{,}454{,}182.81766 \pm 0.00002 + 31.2197874 \pm 0.0000014\, E \text{ days}.$$

Table 6
Light and Velocity Curve Results[a]

Parameter	Symbol	Value
Period (days)	P	31.2197874 ± 0.0000014
Epoch of primary eclipse minimum (HJD)	T_0	$2{,}454{,}162.73553 \pm 0.00002$
Eccentricity	e	0.46659 ± 0.00001
Longitude of periastron (deg)	ω_1	63.7899 ± 0.0008
RV semiamplitude (km s^{-1})	K_1	50.078 ± 0.009
RV semiamplitude (km s^{-1})	K_2	50.388 ± 0.009
Systemic velocity (km s^{-1})	γ	5.020 ± 0.036
Semimajor axis ($R_\odot$)	a	54.85 ± 0.05
Inclination (deg)	i	89.825 ± 0.003
Mass ratio	M_2/M_1	0.9938 ± 0.0002
Surface potential	Ω_1	53.413 ± 0.019
Surface potential	Ω_2	53.832 ± 0.024
Temperature (K) (fixed)	T_1	$5900^{b} \pm 100$
Temperature (K)	T_2	5843 ± 100
Luminosity ratio	$L_1/(L_1+L_2)_y$	0.5174 ± 0.0014
Luminosity ratio	$L_1/(L_1+L_2)_b$	0.5191 ± 0.0015

Notes.

[a] Wilson–Devinney simultaneous solution, including proximity and eclipse effects, of the light and velocity data.

[b] Adopted value, see the text.

Table 7
Fundamental Parameters of HD 74057

Parameter	Primary	Secondary
M ($M_\odot$)	1.138 ± 0.003	1.131 ± 0.003
R ($R_\odot$)	1.064 ± 0.002	1.049 ± 0.002
$\log g$ (cm s^{-2})	4.441 ± 0.004	4.450 ± 0.004
M_{bol} (mag)	4.517 ± 0.004	4.589 ± 0.004
$L/L_\odot$	1.232 ± 0.005	1.152 ± 0.005
y (mag)	7.905 ± 0.003	7.981 ± 0.003
b (mag)	8.280 ± 0.003	8.363 ± 0.003
Spectral type	G0 dwarf	G0 dwarf
v_{rot} (km s^{-1})	6.4 ± 1.0	6.5 ± 1.0

Given the limited timespan of our data set, we made no attempt with the WD program to search for any period change.

7. SPECTRAL TYPES AND SPECTROSCOPIC MAGNITUDE DIFFERENCE

To determine spectral types of late-type stars, Strassmeier & Fekel (1990) identified several luminosity-sensitive and temperature-sensitive line ratios in the 6430–6465 Å region. Those line ratios plus the general appearance of the spectrum were employed as spectral-type criteria. However, for stars earlier than early-G spectral class, the line ratios in the 6430 Å region have little sensitivity to luminosity.

For HD 74057 the similar line strengths of the components and the near unity mass ratio indicate that the two spectral types are also very similar. With $B-V = 0.598$ (Perryman & ESA 1997) for the combined system, both stars are slightly hotter than the Sun. Thus, we compared the spectrum of HD 74057 with those of late-F and early-G dwarfs primarily taken from the lists of Keenan & McNeil (1989) and Fekel (1997). Spectra of those reference stars were obtained at KPNO with the same telescope, spectrograph, and detector as our spectra of HD 74057. With a computer program developed by Huenemoerder & Barden (1984) and Barden (1985), various combinations of reference-star spectra were rotationally broadened, shifted in radial velocity, appropriately weighted, and added together in an attempt to reproduce the spectrum of HD 74057 in the 6430 Å region. We obtained an excellent fit to its spectrum with the slightly metal-rich solar-type star HR 937 (G0 V (Keenan & McNeil 1989) and [Fe/H] = +0.07 (Taylor 2005)) used for both components. Thus, the iron abundance of the reference star HR 937 indicates that HD 74057 has an iron abundance that is somewhat greater than the Sun's.

Because of the G0 spectral class of both components, we determined their luminosity classes from their absolute visual magnitudes computed with the *Hipparcos* parallax, as revised by van Leeuwen (2007). We did not apply a correction for interstellar reddening due to the nearness of the system. The absolute magnitudes indicate that both stars are dwarfs.

The resulting continuum-intensity ratio $I_2/I_1 = 0.9685$. Because of the similarity of the spectral types, we adopt this value as the luminosity ratio, which corresponds to a magnitude difference in the 6430 Å region of 0.03 mag with an estimated uncertainty of 0.1 mag. This result is in reasonable agreement with the more precise determination of 0.07 mag for the Strömgren y-band magnitude difference from the light curve solution (see Table 7).

8. MAGNITUDES AND DISTANCE

Olsen (1983) determined the apparent magnitude and color indices for HD 74057 to be $y = 7.190 \pm 0.005$, $b-y = 0.378 \pm 0.003$, $m_1 = 0.188 \pm 0.004$, and $c_1 = 0.342 \pm 0.004$, respectively, for the maximum amount of combined light outside eclipse. From the WD solution one obtains the bolometric magnitudes, the luminosity of the system, and the individual luminosity ratios (see Tables 6 and 7). The appropriate bolometric correction for a 5900 K main-sequence star is −0.060 mag (Flower 1996), giving $M_y = 4.577 \pm 0.004$. The luminosity ratio of 0.935 in the y bandpass equates to 0.717 mag, and therefore the apparent magnitude for the primary is 7.907 ± 0.012 mag. From the absolute and apparent magnitudes, the computed distance is 46.3 ± 0.3 pc. The original *Hipparcos* parallax is $0\farcs02062 \pm 0\farcs00095$ (Perryman & ESA 1997) which has been revised to $0\farcs01990 \pm 0\farcs00056$ by van Leeuwen (2007). The corresponding distances are 48.5 ± 2.2 pc and 50.3 ± 1.4 pc.

9. CIRCULARIZATION AND SYNCHRONIZATION

The two main theories of orbital circularization and rotational synchronization (e.g., Zahn 1977; Tassoul & Tassoul 1992) disagree significantly on absolute timescales but do agree that synchronization should occur first. Duquennoy & Mayor (1991) examined the multiplicity of solar-type stars in the solar neighborhood. They determined that, while systems with periods $\leqslant$10 days had circular orbits, longer period orbits are generally eccentric. HD 74057 has a period of 31.2 days and its components are dwarfs, so it is not particularly surprising that it has a significantly eccentric orbit.

Hut (1981) has shown that in an eccentric orbit the rotational angular velocity of a star will tend to synchronize with that of the orbital motion at periastron, which is called pseudosynchronous rotation. With Equation (42) of Hut (1981), we compute a pseudosynchronous period of 12.68 days for HD 74057. Combining that period with the radii from the light curve solution produces pseudosynchronization rotational velocities of 4.4 and 4.1 km s^{-1}.

To see if the components are pseudosynchronously rotating, we have determined projected rotational velocities from our red-wavelength KPNO spectra with the procedure of Fekel (1997). For early-G stars, a value of 3 km s^{-1} was adopted for the macroturbulent velocity. To convert the observed v sin i values into equatorial rotational velocities, we assume, as is generally done, that the orbital and rotational axes are parallel, so the inclinations are equal. The v sin i values, averaged from 20 spectra, are 6.4 and 6.5 km s^{-1} for the primary and secondary, respectively. Both values have an estimated uncertainty of ±1.0 km s^{-1}. The orbital inclination is so close to 90° that we simply adopt the v sin i values as the equatorial rotational velocities. Thus, both components are rotating about 50% faster than their pseudosynchronous values.

Zahn (1977, 1989) examined the mechanism of turbulent dissipation for producing tidal friction in stars with convective atmospheres. Equation (6.1) of Zahn (1977), involving the stellar mass ratio, the stellar radius, and the semimajor axis of the binary, can be used to estimate a timescale for synchronization. However, we have shown that HD 74057 has a very eccentric orbit, and so the rotational velocity will tend to synchronize with the orbital motion at periastron (Hut 1981). Thus, in the formulation of Zahn (1977) we have replaced the semimajor axis, a, with the periastron separation, $a(1-e)$. This results in a

pseudosynchronization timescale of 0.44 Gyr. Claret & Cunha (1997) compared the theoretical predictions of Zahn (1977, 1989) with observational results for eclipsing binaries and found that the components on average are pseudosynchronized, but some systems do have rotational velocities that are very different from the theoretical predictions.

Combining our photometric rotation period of 8.4 days with our v sin i values for both components results in radii of 1.07 and 1.09 $R_\odot$ for the primary and secondary, respectively. These values are in excellent agreement with the radii of 1.064 and 1.049 $R_\odot$ from our light curve solution. This supports our assumption that the rotational and orbital axes are parallel.

10. EVOLUTIONARY STATUS

Clausen et al. (2009) compared eleven F, G, and K dwarf binaries with very well determined masses and radii to isochrones that were computed from Yale-Yonsei evolutionary models with solar composition (Yi et al. 2001; Demarque et al. 2004). Their Figure 10 shows that while some binary pairs produce consistent ages in the mass–radius plane, others do not, presumably because of enhanced stellar activity and its effect on envelope convection in stars less massive than the Sun (Ribas et al. 2008). With masses of 1.1 $M_\odot$, the components of HD 74057 appear to be too massive to be significantly affected by their chromospheric activity. Placing the components of HD 74057 in that mass–radius figure results in an age between 0.5 and 1.0 Gyr for the system. Unfortunately, the masses and radii of the components of HD 74057 are so similar that they provide little leverage on the age consistency of the components. In Figure 7, we plot the components of HD 74057 in a theoretical H-R diagram, comparing the stellar pair with the luminosities and effective temperatures of two Yale-Yonsei evolutionary tracks. Those tracks have been constructed for a mean component mass of 1.134$M_\odot$ because the two masses of HD 74057 are so similar. The abundances used for the evolutionary tracks, $Z = 0.018$ and $Z = 0.031$, correspond to solar metallicity and a metallicity of [Fe/H] = 0.2, respectively. It is clear that the best fit to the components in the luminosity–effective-temperature plane is for [Fe/H] = 0.2. Both components are at the base of this metal-rich evolutionary track and close to the zero-age main sequence, indicating an age of about 1.0 Gyr. Such a young age is consistent with the moderate rotation of the components and photometric variability due to starspots. However, that age is roughly a factor of two greater than the estimated timescale for pseudosynchronous rotation, and the components are not yet pseudosynchronized.

11. SUMMARY

We analyzed new Strömgren *by* photometric observations and double-lined radial velocities with the WD program and determined the orbital elements and absolute dimensions of the eclipsing solar-type binary HD 74057. From the combined solution, the orbital period is 31.2197874 ± 0.0000014 days and the eccentricity is 0.46659 ± 0.00001. Despite the relatively long period, the orbit has a very high inclination of 89.°825 ± 0.°003; therefore, the system is seen almost perfectly edge on. We find that the system is a detached binary with almost identical G0 dwarf components. Their masses are $M_1 = 1.138 \pm 0.003\,M_\odot$ and $M_2 = 1.131 \pm 0.003\,M_\odot$, while the radii are $R_1 = 1.064 \pm 0.002\,R_\odot$ and $R_2 = 1.049 \pm 0.002\,R_\odot$. Using the results of our WD solution, we compute a distance to the system of 46.3 ± 0.3 pc, which is 9% smaller than the revised *Hipparcos* value of van Leeuwen (2007). The stars are rotating about 50% faster than their predicted pseudosynchronous velocities. A comparison with evolutionary tracks indicates that the stars are somewhat metal rich and have an age of about 1.0 Gyr.

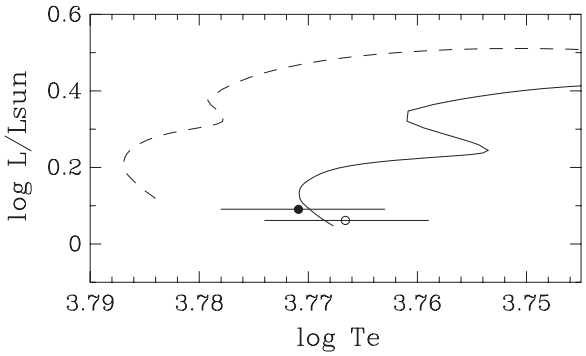

Figure 7. Positions of the two components of HD 74057 (primary: filled circle; secondary: open circle) in a theoretical H-R diagram compared with the Yonsei-Yale evolutionary tracks. The dashed line corresponds to a track for the mean mass of the components ($M = 1.134\,M_\odot$) and solar metallicity, while the solid line results from the same mass but a metallicity of $Z = 0.031$ or [Fe/H] = 0.2.

Astronomy at Tennessee State University is supported by NASA, NSF, Tennessee State University, and the state of Tennessee through its Centers of Excellence programs. We thank Walter Van Hamme for advice regarding the WD program and for computing the error bars of the parameters of the final solution. This research made use of the SIMBAD database, operated at CDS, Strasbourg, France.

REFERENCES

Allen, C. W. 2000, in Allen's Astrophysical Quantities, ed. A. N. Cox (New York: Springer), 388
Alonso, A., Arribas, S., & Martínez-Roger, C. 1996, A&A, 313, 873
Barden, S. C. 1985, ApJ, 295, 162
Barker, E. S., Evans, D. S., & Laing, J. D. 1967, R. Obs. Bull., 130, 355
Claret, A., & Cunha, N. C. S. 1997, A&A, 318, 187
Clausen, J. V., Bruntt, H., Claret, A., et al. 2009, A&A, 502, 253
Davies, D. 2006, Perem. Zvezdy, 6, 14
Davies, D. 2007, Perem. Zvezdy, 6, 16
Demarque, P., Woo, J.-H., Kim, Y.-C., & Yi, S. K. 2004, ApJS, 155, 667
Duquennoy, A., & Mayor, M. 1991, A&A, 248, 485
Fekel, F. C. 1997, PASP, 109, 514
Fitzpatrick, M. J. 1993, in ASP Conf. Ser. 52, Astronomical Data Analysis Software and Systems II, ed. R. J. Hanisch, R. V. J. Brissenden, & J. Barnes (San Francisco, CA: ASP), 472
Flower, P. J. 1996, ApJ, 469, 355
Henry, G. W. 1999, PASP, 111, 845
Henry, G. W., Fekel, F. C., & Hall, D. S. 1995, AJ, 110, 2926
Huenemoerder, D. P., & Barden, S. C. 1984, BAAS, 16, 510
Hut, P. 1981, A&A, 99, 126
Keenan, P. C., & McNeil, R. C. 1989, ApJS, 71, 245
Kurucz, R. L. 1993, in Light Curve Modeling of Eclipsing Binary Stars, ed. E. F. Milone (New York: Springer), 93
Lucy, L. B. 1967, Z. Astrophys., 65, 89
Olsen, E. C. 1983, A&AS, 54, 55
Perryman, M. A. C., & ESA 1997, The *Hipparcos* and *Tycho* Catalogues (ESA SP-1200; Noordwijk: ESA)
Ribas, I., Morales, J. C., Jordi, C., et al. 2008, Mem. Soc. Astron. Ital., 79, 562
Rossiter, R. A. 1924, ApJ, 60, 15
Scarfe, C. D., Batten, A. H., & Fletcher, J. M. 1990, Publ. Dom. Astrophys. Obs., 18, 21
Strassmeier, K. G., & Fekel, F. C. 1990, A&A, 230, 389
Tassoul, J.-L., & Tassoul, M. 1992, ApJ, 395, 259
Taylor, B. J. 2005, ApJS, 161, 444
Van Hamme, W. 1993, AJ, 106, 2096
Van Hamme, W., & Wilson, R. E. 1984, A&A, 141, 1

Van Hamme, W., & Wilson, R. E. 1985, Ap&SS, 110, 169
Van Hamme, W., & Wilson, R. E. 2003, in ASP Conf. Ser. 298, GAIA Spectroscopy, Science and Technology, ed. U. Munari (San Francisco, CA: ASP), 323
Van Leeuwen, F. 2007, *Hipparcos*, The New Reduction of the Raw Data (Astrophysics and Space Science Library, Vol. 350; Berlin: Springer)
Wilson, R. E. 1979, ApJ, 234, 1054
Wilson, R. E. 1990, ApJ, 356, 613
Wilson, R. E., & Devinney, E. J. 1971, ApJ, 166, 605
Wolfe, R. H., Horak, H. G., & Storer, N. W. 1967, in Modern Astrophysics, ed. M. Hack (New York: Gordon & Breach), 251
Yi, S. K., Demarque, P., Kim, Y.-C., et al. 2001, ApJS, 136, 417
Zahn, J.-P. 1977, A&A, 57, 383
Zahn, J.-P. 1989, A&A, 220, 112